Measurement of the Di–jet Cross-Section and the Effective Parton Density of the Photon at HERA.

Tania R. Ebert
(for the H1 Collaboration)

Oliver Lodge Laboratory, University of Liverpool, P.O. Box 147, Liverpool, L69 3BX, U.K.

Abstract.
A measurement of the double differential di–jet cross-section in photoproduction processes using data from the H1 experiment at HERA is presented. The effective leading order parton density function of the photon is determined. The result shows a scale dependence compatible with the prediction from perturbative QCD.

INTRODUCTION

The probability of finding a quark in the photon is predicted by perturbative QCD to be [1]:

$$f_{q/gamma} \propto \ln \mu_f \tag{1}$$

where μ_f is the factorisation scale at which the photon is probed. The form of this expression reflects the anomalous component of the photon, and is distinctly different from hadronic parton distributions.

In this analysis, the inclusive double differential di-jet cross-section in photoproduction is measured. This is used to determine an effective parton density function of the photon and subsequently to test the relation 1.

DI–JET CROSS SECTION

In leading order, the di–jet cross–section can be expressed with four components:

$$\frac{\mathrm{d}^4\sigma}{\mathrm{d}y\mathrm{d}x_\gamma\mathrm{d}x_p\mathrm{d}\cos\theta^*} \sim \sum_{ij} \frac{f_{\gamma/e}}{y}\frac{f_{i/\gamma}}{x_\gamma}\frac{f_{j/p}}{x_p} \mid M_{ij}(\cos\theta^*) \mid^2 \tag{2}$$

The first term on the right hand side of equation 2 is the probability of finding a photon with energy yE_e in the electron, the second (third) term is the probability of finding a parton $i(j)$ in the photon (proton) with energy $x_\gamma E_\gamma$ ($x_p E_p$) and the last term is the QCD matrix element, describing the distribution of the parton scattering angle θ^* in the parton–parton centre of mass frame.

Conventionally, the renormalisation (μ_r) and factorisation (μ_f) scales are taken to be equal to the transverse momentum p_T of the scattered partons. In leading order, p_T can be expressed in terms of the four observables in (2):

$$p_T^2 = \frac{1}{4} s_{ep} y x_\gamma x_p \sin^2\theta^* \tag{3}$$

where s_{ep} is the ep centre of mass energy.

In photoproduction events, additional interactions between the photon and proton remnants may occur, giving rise to additional energy in the event, uncorrelated with the jets from the hard subprocess [3]. The effects of these multiple interactions therefore need to be taken into account before conclusions about $f_{i/\gamma}$ can be drawn from the data.

In this analysis the PYTHIA event generator [2] is used to determine the parton–hadron correlations. It contains a model for multiple interactions and has been shown to give a good description of the underlying event energy observed in the data [3]. Although a leading order generator, it simulates higher order effects by parton showers, and has also been shown [4] to describe distributions in the data which are sensitive to such effects.

RESULTS

A detailed description of the H1 detector can be found elsewhere [5]. The analysis is based on data taken in 1994, corresponding to an integrated luminosity of 2 pb^{-1} . Photoproduction events were selected by requiring that the scattered electron is not detected in the central detector, therefore restricting the photon virtuality to $Q^2 < 4\,\mathrm{GeV}^2$. The kinematic region was restricted to $0.2 < y < 0.83$.

A cone algorithm [6] with cone size $R = 0.7$ was used to reconstruct the jets. Jets with transverse energy $E_T > 8\,\mathrm{GeV}$ and rapidity $-0.5 < \eta < 2.5$ were accepted. In addition, the rapidity difference between the jets was required to satisfy $\Delta\eta < 1$ which is equivalent to restricting $|\cos\theta^*| < 0.46$.

The differential di–jet cross–section was integrated over y and $\cos\theta^*$, and is presented as a function of the E_T of the second highest E_T jet, and x_γ^{jets} which is reconstructed from the two highest E_T jets in the event:

$$x_\gamma^{jets} = \frac{E_T^{jet1} e^{-\eta^{jet1}} + E_T^{jet2} e^{-\eta^{jet2}}}{2 y_{jb} E_e} \tag{4}$$

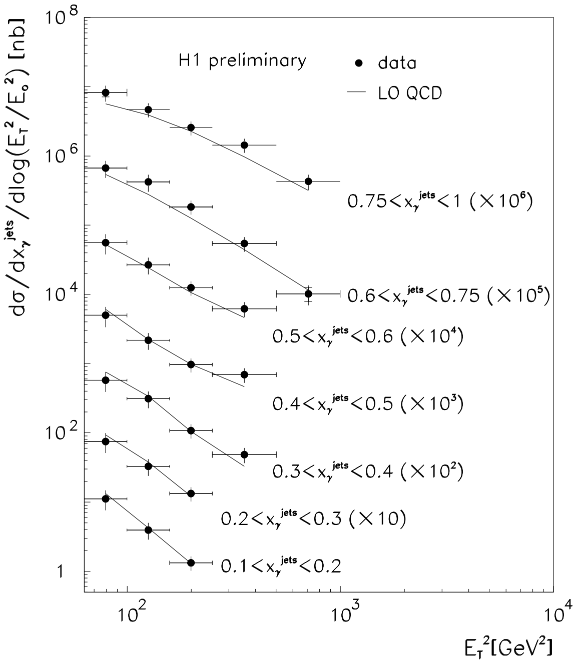

FIGURE 1. The differential di–jet cross section as a function of E_T and x_γ^{jets} in the range $Q^2 < 4\,\mathrm{GeV}^2$ and $0.2 < y < 0.83$. The data(points) are compared to the leading order calculation from the PYTHIA generator using GRV-LO parton densities for the photon and proton.

The cross-section was corrected for detector effects using an unfolding procedure [7]. At this stage no corrections were applied for the underlying event energy. The largest contribution to the systematic error arises from the uncertainty in the knowledge of the hadronic energy scale of the calorimeter. The result is shown in figure 1. The data is compared to the prediction from the PYTHIA model with multiple interactions using GRV-LO parton density functions for both the photon and proton [8,9]. Overall, the description of the data is good, except at high x_γ and high E_T.

EFFECTIVE PARTON DENSITY OF THE PHOTON

The concept of an effective parton density function was developed by Combridge and Maxwell [10]. It is based on the fact that the shapes of the leading order matrix elements for the three dominant contributions to the di–jet cross-section ($qq \to qq$, $qg \to qg$ and $gg \to gg$) are very similar, although they differ in normalisation due to the different colour factors involved. A single effective

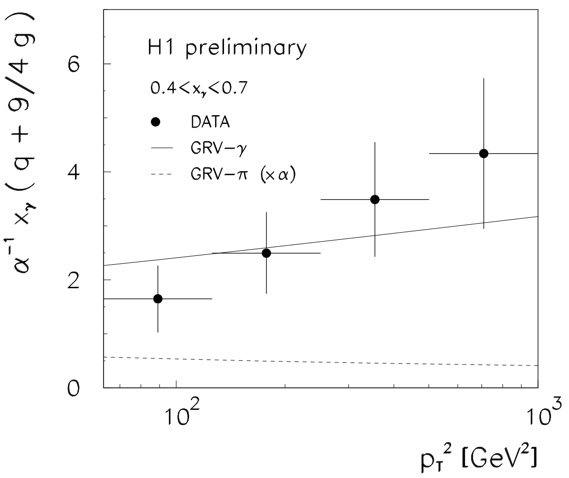

FIGURE 2. The leading order effective parton distribution of the photon $x_\gamma \tilde{f}_\gamma = x_\gamma(q + 9/4g)$ normalised to the fine structure constant α, for $0.4 < x_\gamma < 0.7$ as a function of the parton p_T^2. The data (points) are compared to the effective parton density functions from the GRV parameterisations of the photon (solid line) and the pion (dashed line).

sub-process (SES) is thus defined, with matrix element $\mid M_{SES} \mid^2 \approx \mid M_{qq} \mid^2$. The quark and gluon distributions are then combined into effective parton distribution functions $\tilde{f}$:

$$\tilde{f}(x) = \sum_q [q(x) + \bar{q}(x)] + \frac{9}{4} g(x) \tag{5}$$

Equation 2 then becomes:

$$\frac{\mathrm{d}^4\sigma}{\mathrm{d}y \mathrm{d}x_\gamma \mathrm{d}x_p \mathrm{d}\cos\theta^*} \sim \frac{f_{\gamma/e}}{y} \frac{\tilde{f}_\gamma}{x_\gamma} \frac{\tilde{f}_p}{x_p} \mid M_{SES}(\cos\theta^*) \mid^2 \tag{6}$$

The measured di–jet cross-section was corrected to a leading order di–parton cross-section by an unfolding procedure [7]. In this way, fragmentation, higher order QCD effects and the underlying event energy were corrected for. The uncertainty in the correction for the underlying event energy was determined by varying the relevant parameters in PYTHIA and repeating the correction procedure. The effective parton density function of the photon $\tilde{f}_\gamma$ was determined by comparing the measured di–parton cross-section with that calculated by PYTHIA using the GRV-LO photon structure function.

The result is shown in figure 2 as a function of the scale p_T^2. The data correspond to the range $0.4 < x_\gamma < 0.7$. In this region, photon structure is dominated by quarks. Also shown are the effective parton densities derived from the GRV parameterisations of the photon [8], which is in good agreement with the data, and of the pion [11], which does not show the same scale dependence as the data. The increase with p_T^2 seen in the data is compatible with the logarithmic dependence of $f_{q/\gamma}$ on the scale μ_f which is predicted by perturbative QCD, and disfavours a typical hadronic parton density of the photon.

CONCLUSIONS

The first measurement of the double differential di-jet cross-section as a function of x_γ and E_T from H1 photoproduction data has been presented. From this, the effective parton density of the photon has been determined. It shows an increase with the scale p_T^2 compatible with the logarithmic dependence predicted by perturbative QCD.

ACKNOWLEDGEMENTS

I would like to thank H. Rick and M. Erdmann for informative discussions on this work.

REFERENCES

1. E. Witten, Nucl. Phys. **B120** (1977) 189.
2. H1 Collaboration, S. Aid et al., Z. Phys. **C70** (1996) 17.
3. T. Sjöstrand, CERN-TH-6488, Comp. Phys. Comm. **82** (1994) 74.
4. H. Rick, "Multiple Parton Interactions and Initial State Parton Radiation in Photoproduction", Proceedings of DIS96, Rome, April 1996, p. 293.
5. H1 Collaboration, I. Abt et al., Nucl. Instr. and Meth. **A386** (1997) 310 and **A386** (1997) 348.
6. J.E. Huth et al., Fermilab-Conf-90/249-E (1990)
7. G. D'Agostini, Nucl. Instr. and Meth. **A362** (1995) 487.
8. M. Glück, E. Reya and A. Vogt, Phys. Rev. **D46** (1992) 1973.
9. M. Glück, E. Reya and A. Vogt, Z. Phys. **C43** (1992) 127.
10. B.L. Combridge and C.J. Maxwell, Nucl. Phys. **B239** (1984) 429.
11. M. Glück, E. Reya and A. Vogt, Z. Phys. **C43** (1992) 651.